# Role of nuclear tunneling in aqueous ferrous–ferric electron transfer

J. S. Bader, R. A. Kuharski, and D. Chandler

Citation: J. Chem. Phys. **93**, 230 (1990); doi: 10.1063/1.459596
View online: http://dx.doi.org/10.1063/1.459596
View Table of Contents: http://jcp.aip.org/resource/1/JCPSA6/v93/i1
Published by the American Institute of Physics.

# Role of nuclear tunneling in aqueous ferrous–ferric electron transfer

J. S. Bader, R. A. Kuharski,[a] and D. Chandler
*Department of Chemistry, University of California, Berkeley, Berkeley, California 94720*

(Received 15 December 1989; accepted 23 March 1990)

By computer simulation and also by analytical methods we have computed the nuclear tunneling enhancement of the rate for ferrous–ferric exchange in water. The model we have examined is the one studied earlier where we treated water as a classical liquid [R. A. Kuharski, J. S. Bader, D. Chandler, M. Sprik, M. L. Klein, and R. W. Impey, J. Chem. Phys. **89**, 3248 (1988)]. But now we treat water quantum mechanically and find that the tunneling enhancement is a factor of 60 in the rate constant. Further, as observed experimentally, we find that the isotope shift on the rate when changing from $D_2O$ to $H_2O$ is approximately a factor of 2. The computer simulation aspects of these calculations employ path integral methods and a novel partitioning of the free energy associated with electron transfer. Our results show that it is insufficient to quantize only the atoms composing the ligands. The quantum dynamics of water molecules beyond the first solvation shell prove quite significant.

## I. INTRODUCTION

Through quantum Monte Carlo calculations, we have examined the role of nuclear tunneling on the electron transfer rate for the aqueous ferrous–ferric exchange. In this paper, we describe the methods employed and the results obtained. Our finding is that the role of tunneling is remarkably large. Indeed, we have discovered that due to the quantal nature of liquid water the rate of electron transfer is 60 times larger than obtained if water is treated classically. Further, in our simulations, the rate is roughly twice as fast in $H_2O$ than in $D_2O$. This particular result is in agreement with the experimentally observed[1] isotope effect for the aqueous $Fe^{3+}$–$Fe^{2+}$ electron transfer.

As described in Sec. III, we consider the model for this system developed by Kuharski *et al.*[2] Specifically, our simulations consider two equivalent $Fe^{3+}$ ions, several hundred water molecules, and an electron. The electron is localized on one of the two ions, or in a resonant state with charge distributed simultaneously on both ions. Our earlier studies have shown that the tight-binding two-state description of the electronic states is very accurate in this model.[2] Further, our estimates of the Landau–Zener adiabaticity parameter[3] show that it is small, $\sim 0.03$. Therefore, the rate of transitions for a fixed interionic separation is well described by the golden rule formula[4]

$$k=\frac{2\pi}{\hbar}K^2\int_{-\infty}^{\infty}\frac{dt}{2\pi\hbar}C(t) \tag{1.1}$$

where

$$C(t)=Q_A^{-1}\,\mathrm{Tr}\exp[-(\beta+it/\hbar)H_A]\exp[(it/\hbar)H_B]. \tag{1.2}$$

Here, as is customary, $\beta$ is $(k_BT)^{-1}$, $2\pi\hbar$ is Planck's constant, $H_A$ refers to the diabatic Hamiltonian for the aqueous system when the electron is localized on ion $A$, $H_B$ is similarly defined, and $Q_A$ is the partition function for diabatic state $A$ insuring $C(0)=1$. The energy $K$ is the resonance energy or coupling matrix element between states $A$ and $B$. It is treated as a constant (i.e., with the Condon approximation) because we have found that for accessible configurations it is only a weak function of solvent nuclear coordinates.[2]

Our calculations and those of others[5] show that the coupling parameter is approximately $k_BT$ for favorable interionic distances of encounter. Therefore, the smallness of the adiabaticity parameter implies a narrow, nearly cusped nuclear potential barrier at the transition state. Hence, significant tunneling contributions to the rate should be expected.

In general, the rate constant can be analyzed with an approach suggested by Gillan.[6] The connection between this approach and a rigorous method for computing quantum rate constants was derived by Voth *et al.*[7] In this method, one computes the reversible work to pull the centroid of the Euclidean time electron path from the vicinity of a stable state (on one of the ions) to the transition state (the point halfway between the ions). The work for such a process, $F^*$, is the activation free energy appearing in the Arrhenius factor for the quantum rate processes.

The golden rule expression leads to this same result as a special case of the general approach. To make the connection explicit, we can follow Wolynes[8] and others[9] who suggest evaluating the time integral (1.1) by stationary phase. From the symmetry of electronic states $A$ and $B$, we note that at pure imaginary time $t^*=i\beta\hbar/2$, $C(t)$ has an extremum on the imaginary time axis, and thus, from assumed analyticity, a stationary phase point. Deforming the contour of integration to pass through the stationary phase point gives by the method of steepest descents

$$k\approx\frac{2\pi}{\hbar}K^2[C(t^*)/2\pi\hbar^2|C''(t^*)|]^{1/2}C(t^*) \tag{1.3}$$

as the reaction rate. If we now express $C(t^*)$ as a path

[a]Current and permanent address is S-Cubed, P. O. Box 1620, La Jolla, CA 92037.

 0021-9606/90/130230-07$03.00 

integral over nuclear coordinates, we observe that $C(t^*)$ is the factor $\exp(-\beta F^*)$ associated with bringing the centroid of the quantum electron to the transition state. Wolynes[8] noted the relationship between $C(t^*)$ and the Arrhenius factor, although he did not make the connection with the more general and rigorous approach. The prefactor in Eq. (1.3) is relatively weakly dependent on solvent quantum mechanics, scaling as $(F^*)^{-1/2}$, and for the aqueous ferrous–ferric reaction we find (see below) its contribution to the tunneling enhancement is almost negligible.

With Eq. (1.3), the rate constant can be analyzed by the methods of equilibrium quantum Monte Carlo. The evaluations of the prescribed free energy changes, however, are not altogether straightforward. The procedure we have devised for this purpose is described in Sec. II. The details and results of the computations are given in Sec. III. Then an analysis of these results employing a harmonic model for the solvent is discussed in Sec. IV, where we also describe our findings in the context of work by others.

## II. METHOD OF CALCULATION

In a path integral representation, using $q$ as shorthand for the coordinates of the solvent, we write

$$C(t^*)=\frac{\int \mathscr{D}q(\tau)\exp\{-S^*[q(\tau)]\}}{\int \mathscr{D}q(\tau)\exp\{-S_A[q(\tau)]\}}\equiv e^{-\beta F^*}, \tag{2.1}$$

where $S_A$ is the action evaluated for the system evolving in diabatic electronic state $A$ for imaginary time $\tau = it$ between 0 and $\beta\hbar$, i.e., when the electron path is

$$r(\tau)=R_A, \qquad 0\leqslant\tau<\beta\hbar, \tag{2.2a}$$

where $R_A$ is the position of ion $A$. Similarly, $S^*$ is the corresponding action with an electron path characteristic of the transition state,

$$\begin{aligned} r(\tau)&=R_A, \qquad 0\leqslant\tau<\beta\hbar/2,\\ &=R_B, \qquad \beta\hbar/2\leqslant\tau<\beta\hbar, \end{aligned} \tag{2.2b}$$

where $R_B$ denotes the position of ion $B$.

The free-energy cost $F^*$ can in principle be calculated by a charging process:

$$F^*=-\beta^{-1}\int_0^1 d\lambda\frac{d}{d\lambda}\times\ln\int\mathscr{D}q(\tau)\exp\{-S_\lambda[q(\tau)]\}, \tag{2.3}$$

where $S_\lambda$ interpolates the action used to weight the paths linearly from the stable state to the transition state value,

$$\begin{aligned} S_\lambda&=S_A+\lambda(S^*-S_A)\\ &=S_A+\lambda\int_0^{\beta\hbar}\frac{d\tau}{\hbar}z(\tau)\{V_B[q(\tau)]-V_A[q(\tau)]\}. \end{aligned} \tag{2.4}$$

Here, $V_A$ is the potential energy evaluated in electronic state $A$, and $V_B$ is similarly defined. With tight-binding, the difference between the two potential energies is $-|e|$ times the difference in the electric potentials at the two ions, and $z(\tau)$ is $\Theta(\tau-\beta\hbar/2)$, where $\Theta(x)$ is the Heaviside function with unit discontinuity at $x=0$. The electron path, then, is effectively described by the one-dimensional variable $z(\tau)$, and $\tau=\beta\hbar/2$ is the imaginary time that the electron moves from ion $A$ to ion $B$. The interactions used to weight configurations in the $\lambda$ ensemble interpolate linearly between their stable and transition state values. For imaginary time $\tau$ between 0 and $\beta\hbar/2$ the solvent interacts with the full electronic charge at ion $A$. From imaginary time $\beta\hbar/2$ to $\beta\hbar$ the solvent interacts with a fictitious charge of $-\lambda|e|$ on ion $B$ and $-(1-\lambda)|e|$ on ion $A$. Only at the endpoints of the integral, $\lambda$ equal to 0 or 1, does the weighting correspond to an actual electron path.

By using Eqs. (2.2)–(2.4), and writing $\langle V_B[q(\tau)]-V_A[q(\tau)]\rangle_\lambda$ as $E_\lambda(\tau)$, we have

$$F^*=\int_0^1 d\lambda\int_0^{\beta\hbar}\frac{d\tau}{\beta\hbar}z(\tau)E_\lambda(\tau). \tag{2.5}$$

Note that because the electronic state is a function of imaginary time, the average solvent polarization $E_\lambda(\tau)$ is as well.

There are a multitude of alternative reversible paths to compute $F^*$. One such path would be to determine the free energy associated with creating an electronic charge distribution consistent with a classical adiabatic transition state, i.e., one which employed in Eq. (2.3) an intermediate $S'_\lambda=(1-\lambda)S_A+\lambda(S_B+S_A)/2$, followed by a second integration from $S'_{\lambda=1}$ to the $S^*$ defined by Eq. (2.2b). A second alternative reversible path to compute $F^*$ would be to directly pull the electron centroid from $R_A$ to $(R_A+R_B)/2$. Zeng *et al.*[10] use this second alternative. In the case of a classical solvent, both of these alternatives as well as the path indicated by Eq. (2.5) are identical and reduce to the procedure employed by Warshel[11] and by Kuharski *et al.*[2] to compute electron transfer activation energies.

To focus on quantum effects, each reversible path is correct, but each is also inconvenient to directly implement numerically. The total activation free energy is a large number, ~20 kcal/mol for this reaction,[2] and the error in its evaluation is likely to be of the same magnitude as the quantum corrections due to nuclear tunneling.

To make further progress, we write $E_\lambda(\tau)$ in terms of its imaginary time-averaged value (zero-frequency imaginary time Fourier mode):

$$E_\lambda^{(0)}=\int_0^{\beta\hbar}\frac{d\tau}{\beta\hbar}E_\lambda(\tau), \tag{2.6}$$

plus the deviation from the average:

$$\delta E_\lambda(\tau)=E_\lambda(\tau)-E_\lambda^{(0)}. \tag{2.7}$$

Defining $z^{(0)}$ and $\delta z(\tau)$ analogously, we see that Eq. (2.5) decouples into contributions from the zero-frequency modes or centroids of the electron and solvent path, and from the deviations of these paths from their average values. The total activation energy can be written as

$$F^*=F_0^*+\delta F^*. \tag{2.8}$$

The first term on the right is the contribution to the activation energy from the zero-frequency modes of the electron and solvent paths,

$$F_0^* = \int_0^1 d\lambda\, z^{(0)} E_\lambda^{(0)}, \tag{2.9}$$

and the second term accounts for the extra change in solvation energy due to quantum modes which have non-zero-frequency in imaginary time,

$$\delta F^* = \int_0^1 d\lambda \int_0^{\beta\hbar} \frac{d\tau}{\beta\hbar} \delta z(\tau) \delta E_\lambda(\tau). \tag{2.10}$$

This breakdown is advantageous for a variety of reasons.

First, as suggested above, a classical bath will have no dispersion in imaginary time, and the only contribution to the activation energy will be from the zero-frequency modes: $F^* = F_0^*$, and $\delta F^*$ is zero. This again implies that, for a classical bath, this algorithm reduces to those employed previously.[2,11] Second, for a quantum solvent characterized by Gaussian statistics and coupled linearly to the electronic state (i.e., the spin-boson Hamiltonian with a polychromatic bath), $F_0^*$ is identical with $F_{\rm cl}^*$, the activation energy for a classical bath with the same Hamiltonian as the quantum system. The entire quantum correction for the spin-boson model must then be $\delta F^*$. In our earlier work on the aqueous ferrous-ferric system, we have found that the harmonic approximation for the solvent polarization modes is quantitatively accurate in predicting activation energies[2] and nearly that accurate in predicting the classical real-time nonequilibrium response to an instantaneous change in electronic state.[12] We expect that the polarization modes of the quantum system are to a good approximation also harmonic and therefore assume that $F_0^*$ is virtually independent of solvent quantum mechanics. For $H_2O$ and $D_2O$ as solvents, then, $\delta F^*$ is almost the entire difference between the activation energy for the quantum solvent and for that of classical water. Rather than subtracting relatively large activation energies we can examine $\delta F^*$ directly. A final benefit of this breakdown is the ease of interpolation. For a harmonic system the integrands in Eqs. (2.9) and (2.10) scale linearly with $\lambda$; for a general system both $E_{\lambda=1}^{(0)}$ and $\delta E_{\lambda=0}(\tau)$ are zero.

## III. SIMULATION DETAILS AND RESULTS

The interactions for our model are those described in Ref. 2. In the quantum simulations described here, we use 430 water molecules, two $Fe^{3+}$ cores, and the electron. The box side length is taken as 23.46 Å to mimic an aqueous solution at low concentration and a water density of 1 g/cc. A cubic spline of 0.5 Å smoothly brings all the interactions to zero at half the box length. We have convinced ourselves[2] that this system is large enough to examine the issues pertinent to electron transfer without significant error due to finite size effects.

The temperature of the system is set at 298 K. The model for $D_2O$ is identical with that for $H_2O$, except that the hydrogen mass is increased from 1 to 2 amu. The ions in the quantum simulation are assumed to be classical species held fixed at a rigid interionic distance of 5.5 Å, close to the most likely distance for electron transfer in this system.[13]

The quantum nature of the solvent is treated using the path integral isomorphism[14] and the Monte Carlo algorithm introduced by Kuharski and Rossky for rigid molecules.[15] Each quantum water becomes a polymer with a number of beads equal to the discretization $P$, each bead itself possessing the six degrees of freedom of a single classical rigid water molecule. The choice $P = 3$ is sufficient to treat the quantum mechanics of pure water.[15] It is clear, however, that not all solvent molecules in our calculations need to be treated quantum mechanically. Water beyond the ionic interaction cutoff, for example, should not significantly influence the activation energy, and their quantum contributions should be correspondingly negligible. Waters in the first shell, conversely, have high-frequency librational and vibrational motions that contribute strongly to the activation energy, and require a discretization even larger than the $P = 3$ value optimal for bulk water. It is convenient, therefore, to select the effective discretization $P$ for a water molecule according to its distance from the electron transfer system.

It is necessary to introduce a bond moving procedure to determine the weighting and hence potential energy of a configuration in which different molecules have different effective discretizations.[16] Suppose a given molecule has $P$ discrete beads and therefore interactions at $P$ points along its imaginary time path. Then the potential used to weight a path of the molecule is

$$V = P^{-1} \sum_{k=1}^{P} V_k, \tag{3.1}$$

where the discrete approximation averages the potential $V_k$ felt at imaginary time $\tau_k = k\beta\hbar/P$. Further, suppose that the value of the potential at time $\tau_k$ is quite close to its value at time $\tau_{k\pm1}$. The sum in Eq. (3.1) may be approximated by

$$V' = (2/P) \sum_{k=1}^{P/2} V_{2k}. \tag{3.2}$$

The intermediate beads do not feel the potential and may be integrated over freely, yielding for computational purposes an effective discretization of $P/2$ rather than $P$. One obvious requirement of this method is that the various values of $P$ for the different regions of solvent be integer multiples.

For purposes of discretization outlined above, the solvent is divided into four regions. Regions 1 and 2 correspond to the first and second solvation shells consisting of 12 and 30 water molecules, respectively. Region 3 contains 278 waters, some of which are beyond the ionic interaction cutoff. Region 4 contains the 110 waters most distant from the ions, all of which are outside of the ionic interaction cutoff. For the results reported here, $P$ for region (1,2,3,4) was first set to (8,4,2,1). Then convergence was tested by doubling the discretizations to (16,8,4,2); the small changes produced in the calculated free energies were within the statistical error of the first results.

TABLE I. Activation free energies[a] and quantum corrections[b] for room-temperature ferrous–ferric exchange in liquid water ($H_2O$) and deuterated water ($D_2O$).

| | Full solvent | Region 1 | Region 2 | Region 3 | Harmonic bath[c] |
|---|---|---|---|---|---|
| $F_0^*$ | 21.4±0.2 | 7.7±0.2 | 7.6±0.2 | 6.1±0.2 | |
| $-\delta F^*(H_2O)$ | 2.41±0.06 | 1.23±0.06 | 0.61±0.08 | 0.57±0.07 | 2.13±0.02 |
| $-\delta F^*(D_2O)$ | 1.86±0.08 | 0.91±0.08 | 0.44±0.08 | 0.51±0.08 | 1.88±0.02 |
| $\Gamma^d$ ($H_2O$) | 65±6 | | | | 41±2 |
| $\Gamma^d$ ($D_2O$) | 25±4 | | | | 26±1 |
| $\nu/\nu_{cl}$ ($H_2O$) | | | | | 1.11±0.01 |
| $\nu/\nu_{cl}$ ($D_2O$) | | | | | 1.10±0.01 |

[a]All free energies in units of kcal/mol. See text for definitions of partial free energies $F_0^*$ and $\delta F^*$, and partitioning into regions 1, 2, and 3.
[b]Error estimates from simulation are ± one standard deviation.
[c]Based on Eq. (4.4) and molecular dynamics determination of $\Phi(\omega)$ for the full bath. The absolute value of $\Phi(\omega)$ is uncertain to a degree associated with the statistical uncertainty in its normalization, Eq. (4.6). The error estimates in this column are due to this uncertainty.
[d]The result of multiplying exp $(-\beta\delta F^*)$ with $\nu/\nu_{cl}$, the latter estimated with the harmonic model.

Because the contribution of a water to the activation energy decreases with its distance from the ions, it is efficient to sample the quantum paths of a molecule in region 1 more often than those of a molecule in region 2, and so on. Equivalently, since it is expected from classical simulations that approximately one-third of the activation energy will come from each of the first three regions,[2] it is most efficient to spend equal amounts of time sampling paths in each of these regions. Since there are fewer molecules in the inner regions, more time per molecule should be spent sampling the paths of these inner shell molecules. The scheme we employ attempts, for each Monte Carlo pass, eight moves of the entire polymer chain and each of its $P$ beads for each water molecule in region 1, four moves for each molecule in region 2, two moves for region 3, and one move for region 4. The sizes of the random translations and rotations were chosen to give $\sim 50\%$ acceptance.

For the equilibrium ($\lambda = 0$) calculations, ten independent configurations were taken from classical molecular dynamics (MD) simulations on this same system equilibrated over long time. The hydrogen mass was set to 1.5 amu and equilibration proceeded for 2500 passes, followed by statistics collection for 500.

Ten independent configurations were again chosen from classical MD with effective charges of (2.5 +) on each ion. These ten configurations from the classical transition state ($\lambda = 1$) ensemble were equilibrated exactly as described above. After equilibration, the hydrogen mass was changed from 1.5 amu to 1 and 2 amu. Equilibration to each new mass lasted 500 passes and was followed by 500 passes of statistics collection for each configuration.

The $\lambda$ integration is accomplished by interpolating $E_\lambda^{(0)}$ and $E_\lambda(\tau)$ linearly in $\lambda$ between the endpoints 0 and 1. The hydrogen mass is assumed not to affect $F_0^*$. Both of these approximations are easily tested by further simulations. As discussed previously, however, these estimates are expected to be quantitatively accurate due to the effectively harmonic behavior of the solvent polarization.

The free energy for locating the electron centroid at the transition state has been computed as outlined above for both $H_2O$ and $D_2O$. The total solvent reorganization free energies are broken down into contributions from each region and are listed in Table I. This breakdown is feasible because the energy, $\delta E_\lambda(\tau)$ in Eq. (2.10), can be partitioned unambiguously into contributions from each molecule in the system. It is evident that each region contributes appreciably to the nuclear tunneling correction as well. The quantum correction enhances the rate by a factor, $\Gamma$, about 60 for $H_2O$. Here, $\Gamma$ is defined as

$$\Gamma \equiv k/k_{cl} = (\nu/\nu_{cl}) e^{-\beta\delta F^*} \simeq e^{-\beta\delta F^*}. \tag{3.3}$$

The quantity $\nu/\nu_{cl}$ is the ratio of frequency factors. As indicated by the last approximate equality, it is roughly unity as shown in Sec. IV. In other words, the quantum contribution to the Arrhenius factor, exp( $-\beta\delta F^*$), is the primary contributor to $\Gamma$.

Previous estimates[17,19(a)] have concentrated solely on the first shell and give $\Gamma$ between 2 and 5, a much smaller factor than we find. It is vital to include more than just the first shell solvent molecules to make a reasonable prediction of $\Gamma$ as seen from Table I.

Due to the nearly harmonic behavior of the bath (see below as well as Ref. 12), $\Gamma$ arises primarily from nuclear tunneling near the transition state region. In this regard, note that the reaction coordinate in our analysis is the electron centroid. Hence, no solvent modes are constrained at the transition state, and no zero-point energy is depleted.

The isotope effect is described by the ratio $\Gamma_H/\Gamma_D$. Our result for this ratio is 2.6±0.5, in reasonable agreement with experiment.[1] As seen from Table I, primary contributions to this isotope effect arise within the first two solvation shells of water, with both shells of similar significance. Note also that in our calculations, intramolecular modes of the molecule are quenched, and internal vibrations appear only implicitly through the effective ion-water pair potentials with rigid water molecules. These potentials produce the correct ferrous and ferric ligand structures. Friedman and Newton,[17(a)] on the other hand, suggest that the quantized ligand O–H and O–D vibrations are a significant contributor to the isotope effect. We do not know what these

vibrations would do if treated rigorously and self-consistently with all the water librations.

## IV. HARMONIC MODEL AND DISCUSSION

Our earlier tests of the harmonic approximation for the solvent polarization showed that Marcus's model of electron transfer is very accurate in the classical regime.[18] We can extend the analysis now to treat the quantum activation energy and $\Gamma$.

The Hamiltonian we consider is the standard spin-boson Hamiltonian

$$H_{SB}=K\sigma_x+\sum_{i=1}^{N}\left(\frac{p_i^2}{2m_i}+\frac{m_i\omega_i^2y_i^2}{2}\right)-\sigma_z\sum_{j=1}^{N}c_jy_j$$
$$=K\sigma_x+H_b(\{y_i\})-\sigma_z\mathscr{E}, \tag{4.1}$$

where $\sigma_x$ and $\sigma_z$ are the Pauli spin matrices and we make the connection that spin $+1$ $(-1)$ corresponds to diabatic electronic state $A$ $(B)$. In accord with the previous definition in Sec. III, we see that the energy difference $E$ can be identified with twice $\mathscr{E}$. The bath Hamiltonian $H_b$ is assumed quadratic in the $N$ normal modes $\{y_i\}$, implying that the solvent coupling $\mathscr{E}$, a linear combination of bath variables, must also obey Gaussian statistics. By defining the spectral density of the bath:

$$\Phi(\omega)=\sum_{i=1}^{N}\frac{\pi\delta(\omega-\omega_i)c_i^2}{m_i\omega_i}, \tag{4.2}$$

we see that the second moment of the solvent coupling (which for a harmonic system fully characterizes the bath fluctuations) may be written as an integral over the spectral density:

$$\langle\mathscr{E}(\tau)\mathscr{E}(\tau')\rangle_b$$
$$=\int_0^\infty\frac{d\omega}{2\pi}\Phi(\omega)\hbar\frac{\cosh\left[(\omega/2)(\beta\hbar-2\tau+2\tau')\right]}{\sinh(\beta\hbar\omega/2)}. \tag{4.3}$$

Here, $\tau$ and $\tau'$ are points in Euclidean (i.e., imaginary) time.

For the spin-boson model, the rate from Eq. (1.2) may be estimated analytically using the stationary phase approximation for the integral. This gives

$$k\approx\frac{2\pi}{\hbar}K^2\left[4\hbar\int_0^\infty d\omega\,\Phi(\omega)\operatorname{cosech}(\beta\hbar\omega/2)\right]^{-1/2}$$
$$\times\exp\left[-2(\pi\hbar)^{-1}\int_0^\infty d\omega\,\Phi(\omega)\omega^{-2}\right.$$
$$\left.\times\tanh(\beta\hbar\omega/4)\right], \tag{4.4}$$

where the argument of the exponential is the activation energy (or free energy—they are identical for a harmonic system) in units of $-k_BT$, and the pre-exponential terms combined are the frequency factor $\nu$. These results are well known.[19]

The spectral density necessary to evaluate these expressions is easily obtained from the cosine transform of the classical real time stable state bath autocorrelation function, since classically we have from Eq. (4.3) that

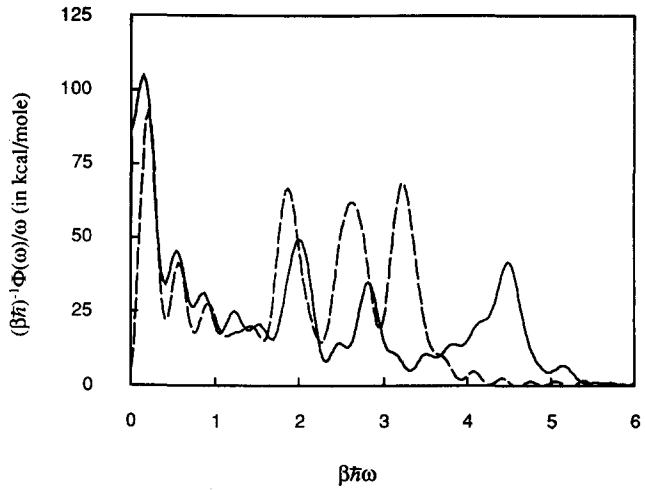


FIG. 1. Quantity $\Phi(\omega)/\omega$ is depicted for liquid $H_2O$ (solid) and $D_2O$ (dash). The spectral density $\Phi(\omega)$ is determined from classical trajectories and normalized according to Eqs. (4.5) and (4.6). The frequency is measured in reduced units of $\beta\hbar\omega$; $\beta\hbar\omega=207\ \mathrm{cm}^{-1}$ at 298 K, the temperature for these simulations.

$$\langle\delta\mathscr{E}(t)\delta\mathscr{E}(t')\rangle_{A\text{ or }B}$$
$$=\beta^{-1}\int_{-\infty}^{\infty}\frac{d\omega}{2\pi}\cos\left[\omega(t-t')\right]\Phi(\omega)/\omega. \tag{4.5}$$

Additionally, $\Phi(\omega)$ satisfies the sum rule

$$\langle E\rangle_A=\frac{2}{\pi}\int_0^\infty d\omega\,\Phi(\omega)/\omega=4F_{cl}^{*}. \tag{4.6}$$

In Ref. 12 we reported the classical real time correlation function for the simulated aqueous $Fe^{3+}$-$Fe^{2+}$ system. In Fig. 1 we show the associated $\Phi(\omega)/\omega$ obtained by Fourier analysis. It is evident that high-frequency modes are present in the classical bath. The quantum correction to the activation energy is found by comparing Eqs. (4.4) and (4.6), i.e.,

$$\beta\delta F^*\approx-\frac{2}{\hbar}\int_0^\infty\frac{d\omega}{\pi}\frac{\Phi(\omega)}{\omega^2}\left[\frac{\beta\hbar\omega}{4}-\tanh\left(\frac{\beta\hbar\omega}{4}\right)\right]. \tag{4.7}$$

The integration (4.7) yields a nuclear tunneling correction to the free energy of 2.1 kcal/mol, which agrees well with our simulation results. The corresponding Arrhenius contribution to the nuclear tunneling factor is predicted by this model to be 36, close to but definitely different from the value of $59\pm6$ obtained by the full quantum simulation.

We have also performed this same harmonic analysis of the $D_2O$ solvent by first computing from a classical MD simulation $\langle\delta E(t)\delta E(0)\rangle_A$ and its corresponding spectral resolution $\Phi(\omega)$. The $\Phi(\omega)/\omega$ for liquid $D_2O$ is plotted and contrasted with that of $H_2O$ in Fig. 1. The calculation of $\delta F^*$ then follows from Eq. (4.7) giving $\exp(-\beta\delta F^*)\approx24$, in good agreement with the full quantum simulation result of $23\pm3$. It is interesting that the harmonic model does better predicting the quantum effects

for liquid $D_2O$ than it does for $H_2O$. Presumably, the reason is that quantal fluctuations are smaller in $D_2O$ than in $H_2O$, and smaller fluctuations probe less of the anharmonic features in the simulated system.

The spectral densities and the pre-exponential factor of Eq. (4.4) provide estimates of the frequency factors. The ratios so obtained are $(\nu/\nu_{cl}) = 1.1$ for both $H_2O$ and $D_2O$.

The harmonic bath analysis is used also by Warshel and Hwang[20] in their "dispersed polaron method." Indeed, Warshel may be the first to exploit in this context the fact that $\Phi(\omega)$ of a complex system can be extracted unambiguously from a classical molecular dynamics trajectory. In some applications by Warshel[21] and by others,[4(b),22] however, a subsequent unnecessary approximation is made in the harmonic analysis. Specifically, a "semiclassical approximation" is made which in effect neglects the commutator $[H_A,H_B]$. This approach gives

$$k_{sc} \approx \frac{2\pi}{\hbar} K^2 \left[ 4\hbar \int_0^\infty d\omega\, \Phi(\omega) \coth(\beta\hbar\omega/2) \right]^{-1/2} \times \exp\left[ -4F_{cl}^{*2} \Big/ \int_0^\infty d\omega\, \Phi(\omega)\hbar\pi^{-1} \times \coth(\beta\hbar\omega/2) \right].$$

The result is correct in the classical limit, but as explained by Siders and Marcus,[19(a)] it leads to an overestimation of the tunneling correction. Qualitatively, the approximation assumes that the barrier to nuclear tunneling is only half its actual width. Stated differently, the approximation replaces the golden rule $\delta$ function of energies with a $\delta$ function in the difference in potentials $V_A - V_B$, and thus replaces the density of the centroid of nuclear paths at the transition state with the actual density of a single point of the nuclear path at the transition state. The two differ by a factor exponentially large in the activation energy.[23] Indeed, when we compute $F_{sc}^*$ from our $\Phi(\omega)$ for $H_2O$, we find that this approximation yields a tunneling correction of 6.6 kcal/mol to the free energy and a corresponding factor of $60–70\times10^3$ in the rate. This prediction does not compare favorably with our simulation results, nor does it predict the experimentally observed isotope effect when used in conjunction with the $D_2O$ spectral density. Therefore, while the harmonic model appears to be a reasonable approximation, the subsequent semiclassical approximation would seem to be unacceptable.

It is the high-frequency motions of liquid water that indicate its quantal nature and lead to the tunneling we observe. In our simulations, these motions are principally librations. The features observed in the spectral density of the simulated system, Fig. 1, are reasonable in light of spectroscopic observations. Specifically, the positions of the high-frequency peaks in Fig. 1 coincide with those observed by IR and Raman measurements for the iron–oxygen stretches and also the wagging and rocking librations of solvated $Fe^{2+}(H_2O)_6$ and $Fe^{3+}(H_2O)_6$.[24] Further, the pure water dielectric response possesses significant density at the high frequencies of Fig. 1.[25] Finally, the shifts in peak location on going from $H_2O$ to $D_2O$ are reasonable in that the librational modes have greater frequency shifts than the stretching modes.

The favorable comparison of the harmonic model with our simulation results for $\Gamma$ serves as a check on the Monte Carlo sampling we have performed. Further, the fact that $\Gamma_H/\Gamma_D$ computed by our simulation agrees well with the experimental isotope effect suggests that our model captures the essential mechanism for that phenomenon in nature. It is reasonable to conclude, therefore, that our remarkable prediction of $\Gamma \approx 60$ is correct. This nuclear tunneling enhancement is an order of magnitude larger than previously imagined.[17,19(a)]

## ACKNOWLEDGMENTS

While carrying out this work, we have benefited from conversations with Rudy Marcus, Marshall Newton, and Arieh Warshel. This research was supported by the United States Department of Energy. Many of the calculations were done on the CRAY X/MP-14 at the University of California, Berkeley. The remainder were performed on a Stellar GS-1000 purchased in part with funding from the National Science Foundation (NSF) and the National Institutes of Health. One of us (J.S.B.) is a NSF Predoctoral Fellow.

[1] J. Hudis and R. W. Dodson, J. Am. Chem. Soc. **78**, 911 (1956) report a factor of 2 as the isotope shift on the aqueous ferrous–ferric rate; T. Guarr, E. Buhks, and G. McLendon, J. Am. Chem. Soc. **105**, 3763 (1983) report an isotope effect of 1.3 for cross reactions involving $Fe_{aq}^{3+/2+}$, yielding a factor of 1.7 as an estimate of the isotope effect for the self-exchange reaction.

[2] R. A. Kuharski, J. S. Bader, D. Chandler, M. Sprik, M. L. Klein, and R. W. Impey, J. Chem. Phys. **89**, 3248 (1988).

[3] J. Ulstrup, *Charge Transfer Processes in Condensed Media* (Springer, Berlin, 1979).

[4] (a) M. Lax, J. Chem. Phys. **20**, 1752 (1952); R. Kubo and Y. Toyozawa, Prog. Theor. Phys. **13**, 160 (1955); (b) N. R. Kestner, J. Logan, and J. Jortner, J. Phys. Chem. **78**, 2148 (1974).

[5] H. L. Friedman and M. D. Newton, Faraday Disc. Chem. Soc. **74**, 73 (1982).

[6] M. J. Gillan, J. Phys. C **20**, 3621 (1987).

[7] G. A. Voth, D. Chandler, and W. H. Miller, J. Chem. Phys. **91**, 7749 (1989).

[8] P. G. Wolynes, J. Chem. Phys. **87**, 6559 (1987).

[9] See, for example, R. P. Van Duyne and S. F. Fischer, Chem. Phys. **5**, 183 (1974); E. Buhks, M. Bixon, J. Jortner, and G. Navon, Inorg. Chem. **18**, 2014 (1979).

[10] C. Zheng, J. A. McCammon, and P. G. Wolynes, Proc. Natl. Acad. Sci. U.S.A. **86**, 6441 (1989).

[11] J.-K. Hwang and A. Warshel, J. Am. Chem. Soc. **109**, 715 (1987).

[12] J. S. Bader and D. Chandler, Chem. Phys. Lett. **157**, 501 (1989).

[13] We have computed ion-ion potentials of mean force for our model of aqueous ferrous–ferric system (work in progress, 1989). When combined with the diabatic state coupling matrix element (Ref. 2), the potential of mean force predicts that electron transfer in this system happens essentially only when the ions are between 5 and 6 Å apart. This prediction is in reasonable agreement with earlier ideas of H. L. Friedman and M. D. Newton, J. Chem. Phys. **76**, 1490 (1982).

[14] D. Chandler and P. G. Wolynes, J. Chem. Phys. **74**, 4078 (1981).

[15] R. A. Kuharski and P. J. Rossky, J. Chem. Phys. **82**, 5164 (1985).

[16] See D. Chandler, in *Liquids, Freezing, and the Glass Transition, Les Houches, Session LI,* edited by D. Levesque, J. P. Hansen, and J. Zinn-Justin (Elsevier, Amsterdam, 1990).

[17] (a) H. L. Friedman and M. D. Newton, J. Electroanal. Chem. **204**, 21 (1986); (b) E. Buhks, M. Bixon, and J. Jortner, J. Phys. Chem. **85**, 3763 (1981).

[18] Here we refer to Refs. 2 and 12 where both equilibrium and dyamical

nonequilibrium aspects of the model were shown to behave as if the solvated redox pair were a two-level system coupled to a harmonic bath. Marcus' predictions for the free energies of electron transfer [R. A. Marcus, J. Am. Chem. Soc. **24**, 966 (1956)] follow from such a Hamiltonian model. The specification of this Hamiltonian is perhaps a somewhat liberal definition of the "Marcus model," however, since Marcus couched his arguments at the level of free-energy functions rather than Hamiltonians.

[19] (a) P. Siders and R. A. Marcus, J. Am. Chem. Soc. **103**, 741 (1981); (b) T. Holstein, Ann. Phys. **8**, 343 (1959). The derivations of Eq. (4.4) found in these papers are equivalent to but perhaps not as direct as the procedure we have outlined. See also Ref. 16. If one begins with Eq. (1.1) for the case that $H_A$ and $H_B$ are harmonic, with the same spectral densities, one finds

$$k=\left(\frac{K}{\hbar}\right)^2 \int_{-\infty}^{\infty} dt \exp\left[\frac{2}{\hbar\pi}\int_0^{\infty} d\omega \frac{\Phi(\omega)}{\omega^2} \times\left[\coth\left(\frac{\beta\hbar\omega}{2}\right)(\cos\omega t-1)+i\sin\omega t\right]\right].$$

See Ref. 4(a). Evaluation of the time integral can be carried out exactly with numerical quadrature. Since the integrand oscillates for real $t$, and the net result of the integral is relatively small, the numerical evaluation is facilitated by displacing the contour so as to be parallel to the real axis and pass through the stationary phase point at $t=i\beta\hbar/2$. For the $\Phi(\omega)$'s shown in Fig. 1, we have carried out such calculations in addition to the analytical stationary phase evaluation, Eq. (4.4). The numerical results so obtained agree with the stationary phase approximation to within 20%.

[20] A. Warshel and J.-K. Hwang, J. Chem. Phys. **84**, 4938 (1986).

[21] A. Warshel, Z. T. Chu, and W. W. Parsons, Science **246**, 112 (1989).

[22] See, for example, J. J. Hopfield, Proc. Natl. Acad. Sci. U.S.A. **71**, 3640 (1974).

[23] W. H. Miller, J. Chem. Phys. **62**, 1899 (1975); G. A. Voth, D. Chandler, and W. H. Miller, J. Phys. Chem. **93**, 7009 (1989).

[24] I. Nakagawa and T. Shimanouchi, Spectrochim. Acta **20**, 429 (1964); S. K. Sharma, J. Chem. Phys. **61**, 1748 (1974); S. P. Best, R. S. Armstrong, and J. K. Beattie, Inorg. Chem. **19**, 1958 (1980); T. E. Jenkins and J. Lewis, Spectrochim. Acta Part **37** A, 47 (1981).

[25] See J. B. Hasted, in *Dielectric and Related Molecular Processes* (Burlington House, London, 1972), Vol. I.